

Supporting Information: *In situ* SAXS Investigation of Vinyl Acetate Polymerization-Induced Self- Assembly

Fabrice Brunel, Paul Galanopoulo, Edgar Espinosa Rodriguez, Muriel Lansalot and Franck
D'Agosto*

Univ Lyon, Université Claude Bernard Lyon 1, CPE Lyon, CNRS, CP2M (UMR 5128), 43 Bvd.
du 11 Novembre 1918, F-69616 Villeurbanne, France

Experimental conditions for *in situ* SAXS monitoring of PEG₄₅-xanthate mediated vinyl acetate emulsion polymerization

The design of an " *in situ* reactor " consistently reproducing the static experiments was required. In this " *in situ* reactor ", part of the polymerization medium flows in a thin wall capillary tube placed under the X-ray beam. The polymerizations were thus performed in a round bottom flask connected to the capillary in which a constant flux of the reaction medium was installed. To do so, a tube was immersed in the three necked round bottom flask through a septum and connected to the capillary via a peristaltic pump. The capillary was then connected back to the flask. In a first step, several experiments were performed to reproduce the results obtained using the static experimental setup. The main challenge with this new " *in situ* reactor " was to maintain the set temperature constant. The temperature of the reaction medium immersed in an oil bath set at 70 °C failed to go above 53 °C once the peristaltic pump was switched on. Part of the medium (≈ 20% of the total dispersion) being in the capillary and the tube were indeed not thermostated. Accordingly, we wrapped the tube into a heating cable and added insulation by covering the part that could not be wrapped with cotton and alumina. 50 mL of a 10 wt% VAc dispersion was subjected to the setup with both the oil bath and the heating cable set at 70 °C. This protocol allowed reaching and maintaining about 60 °C inside the flask after 10 min. Once the setup with the heating cable was validated, we looked to reproduce in this setup the experiment from ref. S1. The experiment however led to only 40% VAc conversion after 100 min while more than 90% was reached in our previous article. We reckoned that this was due to the constant flux toward the capillary. Indeed, as the dispersion flows in the tube with a relatively low diameter (1 mm), high shear forces probably impacted the nucleation. We thus assumed that two key parameters

should be influencing the kinetics: the total volume of reaction medium and the moment the pump was started. On the first hand, we supposed that delaying the start of the pump long enough to let the nucleation proceed would reduce the impact of the flow on this critical stage. Looking at the kinetic profile of the reference experiment, at 25 min the nucleation step should be nearly over. We thus ran two additional syntheses for a total volume of 50 mL, one starting the pump after 20 min and the second after 30 min. However, for the experiment ran with the pump starting after 20 min, the evolution of the VAc conversion failed to reach consistent values with only 60% after 100 min. It still allowed reaching higher conversion than previously. The synthesis performed while starting the pump after 30 min exhibited a kinetic profile similar to the reference synthesis, while only reaching a maximum conversion of 80%. Additionally, it should be noted that, as we aimed to monitor the nucleation step and the transition of morphologies, starting the pump when more than 50% of the monomer has been consumed was not desirable. Increasing the total volume of the reaction medium could allow decreasing the impact of the flow through the tube by decreasing the proportion of the medium transiting through it. By raising the volume to 100 mL and starting the pump after 5 min, VAc conversion of 90% was reached. However, the polymerization rate seemed to be slightly lower, and the nucleation longer compared to the reference (Figure S1). Eventually, a total volume of 100 mL while starting the pump after 10 min led to a kinetic profile that was very similar to that of the reference. Furthermore, the comparison between the results of both experiments targeting the same DP and solid content but using either a conventional or an *in situ* setup yielded approximately the same results in terms of molar mass distribution. The setup and the protocol validated, the *in situ* reactor was brought at the ESRF to perform *in situ* SAXS measurements. However, considering

the conditions dictated by the beamline at the ESRF, some additional adjustments had to be made. Notably, the length of the tube had to be increased so that the capillary could be placed under the X-ray beam. To outweigh the increased volume of liquid in the resulting longer tube, we notably increased the total volume to 200 mL. Several experiments were run at the ESRF but eventually, only one ran for a total volume of 200 mL and targeting a DP of 200 for the PVAc block provided reliable data.

Table S1: Comparison of experimental conditions and the results for the aqueous emulsion polymerization of VAc (target DP of 200) in the presence of a PEG₄₅-X performed either in a conventional or an *in situ* setup. Experiments were performed at 70 °C with [PEG₄₅-X]/[AIBA] = 3.

	m (g)				Solid content ^a	Conversion ^b (%)	M_n (Đ) ^c kg mol ⁻¹
	PEG ₄₅ -X	VAc	AIBA	H ₂ O			
<i>In situ</i>	2.601	19.456	0.103	198.9	9.1	89	16.8 (2.3)
Static	0.2749	20.45	0.0115	20.8	9.1	94	17.9 (2.3)

^a Experimental final solids content measured by gravimetric analysis. ^b Conversion calculated from the solids content. ^c Experimental number-average molar mass and dispersity, M_w/M_n , of the copolymer determined by SEC-THF using a calibration based on PS standards.

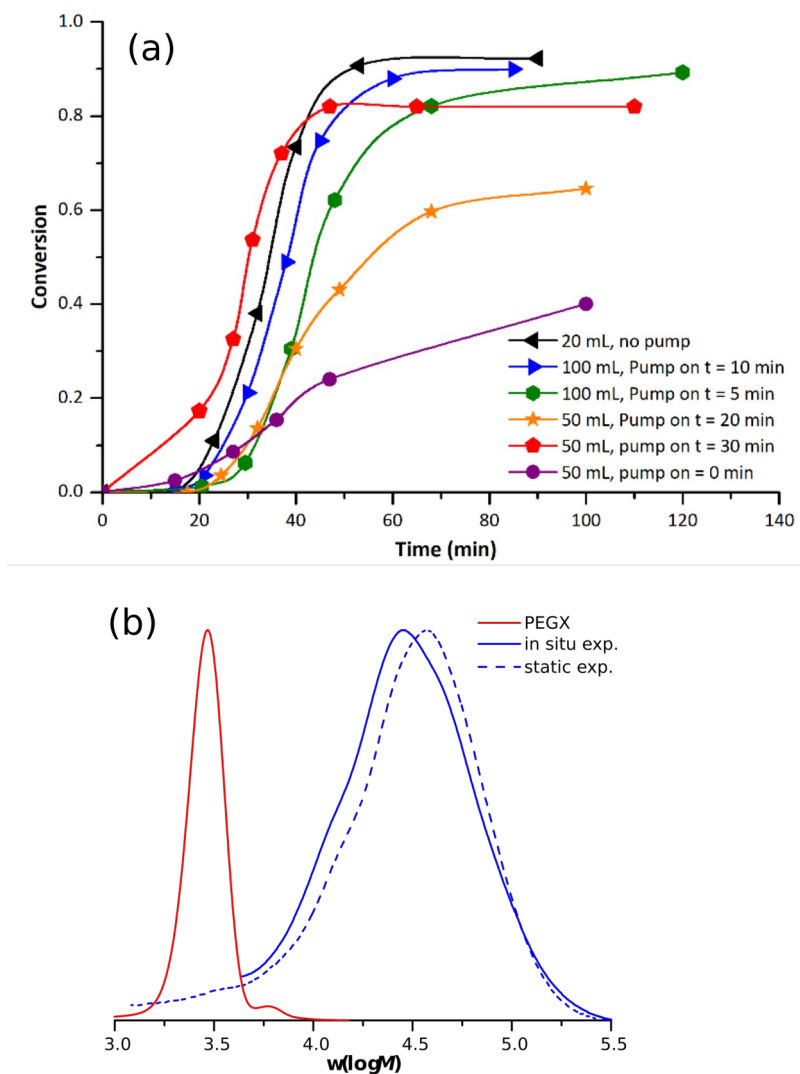


Figure S1: (a) Evolution of conversion versus time for PEG₄₅-X-mediated emulsion polymerization of VAc using the *in situ* reactor. All the experiments were conducted setting the oil bath and heating cable at 70 °C, "20 mL, no pump" is the reference experiment from ref. S1 performed in a conventional reactor. (b) SEC-THF traces of the final PEG₄₅-*b*-PVAc₂₀₀ performed either in a conventional or an *in situ* setup. Experiments were performed at 70 °C with [PEG₄₅-X]/[AIBA] = 3.

Cryo-TEM images

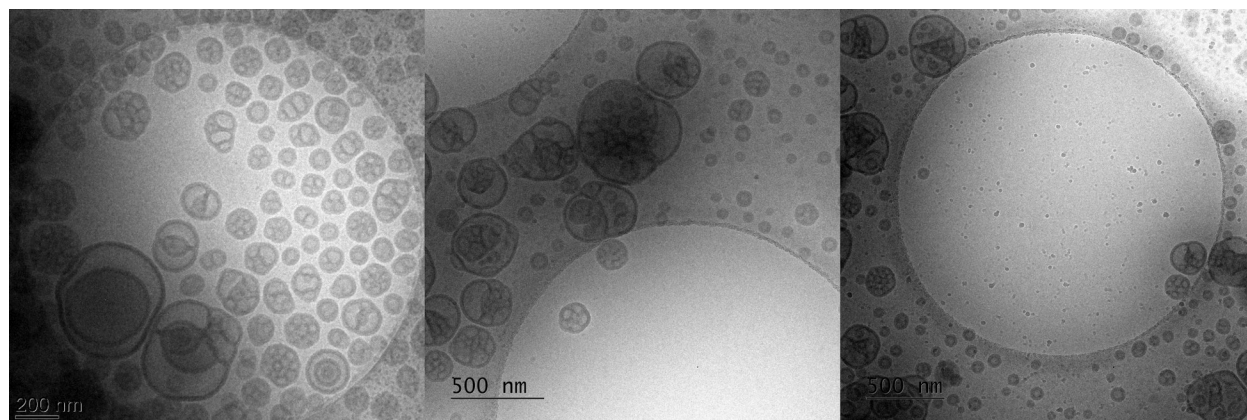


Figure S2: Representative cryo-TEM images of the particles synthesized during the *in situ* experiment.

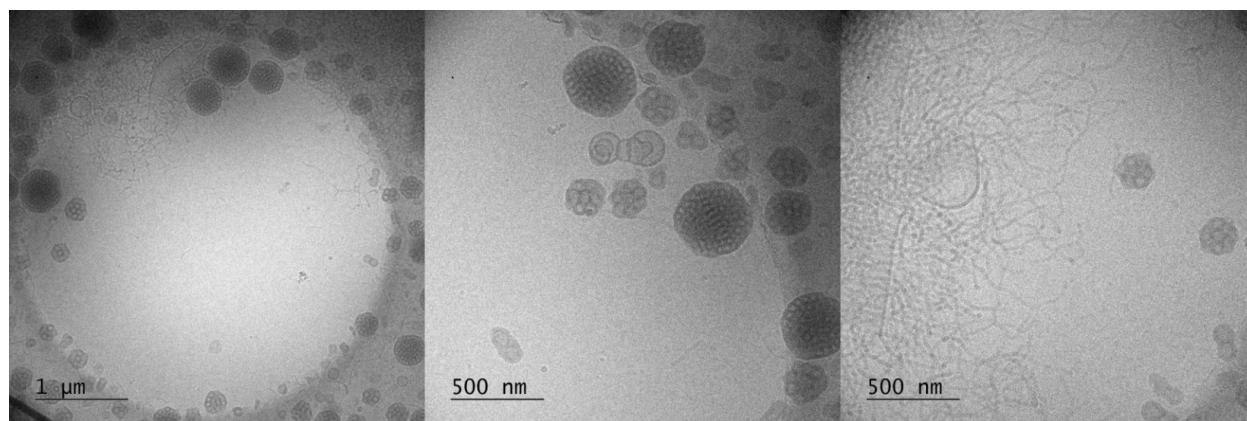


Figure S3: Representative cryo-TEM images of the particles synthesized during the static experiment.^{S1}

SAXS spectra

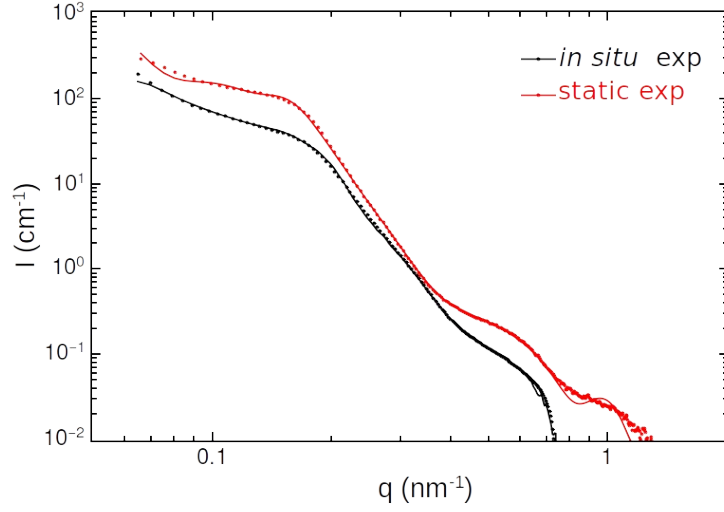


Figure S4: Scattering intensity of the final latexes synthesized during *in situ* and static experiments.

Table S2: Fitting parameters of the final morphologies with polydisperse vesicle form factor (σ R_c , t_{PEG} t_{PVAc} are the polydispersity, the core radius and the thickness of the PEG and PVAc layer) with a hard sphere structure factor of the synthesized particles from *in situ* and static experiments (R_{HS} and ϕ are the Hard sphere radius and the volume fraction).

	Form Factor: Polydisperse vesicles				Structure Factor: Hard spheres	
	σ	R_c (nm)	t_{PEG} (nm)	t_{PVAc} (nm)	R_{HS} (nm)	ϕ
<i>In situ</i>	0.5	30	7.4	9.1	20	0.24
Static	0.3	44.4	8.1	7.3	20.9	0.38

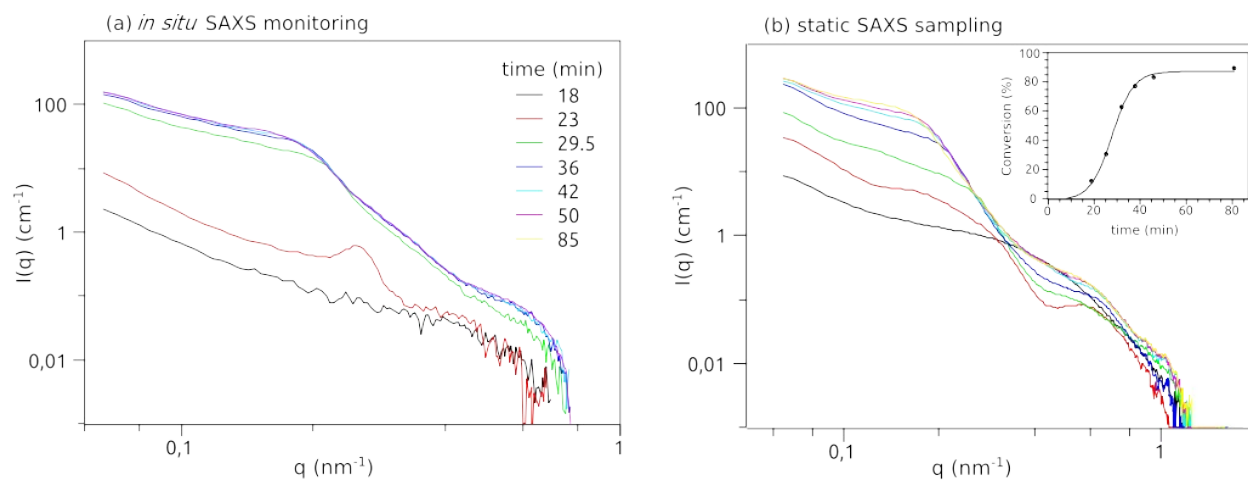


Figure S5: Scattering intensity during the synthesis with (a) *in situ* and (b) static experiments.

Table S3: Fitting parameters (Guinier model) of the morphologies between $t = 18.3$ and 20.2 min. R_g the radius of gyration and I_0 the Guinier constant.

time (min)	Guinier model		Guinier model	
	I_0 (cm^{-1})	R_g (nm)	I_0 (cm^{-1})	R_g (nm)
18.3	4.970	26.8	0.173	5.3
18.5	2.600	22.5	0.172	5.3
18.6	2.252	22.2	0.142	4.8
18.8	1.593	19.6	0.134	5.0
19.0	1.923	23.5	0.173	5.4
19.2	0.966	16.5	0.113	4.6
19.4	0.583	14.4	0.134	4.9
19.6	0.649	13.6	0.110	4.6
19.7	0.537	13.4	0.138	4.7
19.9	0.482	12.6	0.133	4.7
20.1	0.461	11.0	0.097	4.2
20.3	0.387	11.1	0.118	4.2
20.5	0.231	10.5	0.123	4.5

Table S4: Fitting parameters (Guinier model) of the morphologies between $t = 20.1$ and 21.75 min. First Guinier model with a radius of gyration (R_g) and Guinier constant (I_0) plus a fractal structure factor with the radius of the aggregated object (r_0) equal to R_g , ξ the size of the aggregate and D the fractal dimension. Second Guinier model with a radius of gyration (R_g) and Guinier constant (I_0) plus a hard sphere structure factor with the radius of the hard sphere (RHS) equal to R_g and a volume fraction f_p

time (min)	Guinier ^a + S(q) Fractal			Guinier ^b + S(q) Hard sphere	
	I_0	ξ	D	I_0	f_p
20.10	0.51	149	3.10	0.45	0.32
20.29	0.57	89	3.21	0.48	0.30
20.47	0.42	98	3.15	0.42	0.26
20.65	0.47	70	3.22	0.46	0.30
20.84	0.45	79	3.17	0.51	0.32
21.02	0.37	52	3.24	0.50	0.31
21.20	0.32	40	3.22	0.48	0.31
21.39	0.28	26	3.23	0.52	0.30
21.57	0.30	17	3.44	0.55	0.32
21.75	0.33	12	3.87	0.54	0.31

a : $R_g = r_0 = 10$ nm

b : $R_g = \text{RHS} = 6.2$ nm

Table S5: Fitting parameters of the morphologies between $t = 21.9$ and 23.2 min. Generalized Porod model with a constant C and an exponent α . Broad peak model: the peak position is related to the d-spacing as $q_0 = 2\pi/d$, I_0 is the scattering intensity at $q = q_0$ and ξ the correlation length. Guinier model with a radius of gyration (R_g) and Guinier constant (I_0) plus a hard sphere structure factor with the radius of the hard sphere (RHS) equal to R_g and a volume fraction f_p

time (min)	Generalized Porod		Broad peak			Guinier ^b + S(q) Hard sphere	
	C	α	I_0	ξ	q_0	I_0	f_p
21.9	2.98E-04	3.44	0.04	29.24	0.24	0.49	0.31
22.1	3.92E-04	3.39	0.08	27.93	0.25	0.42	0.31
22.3	3.64E-04	3.49	0.11	25.58	0.25	0.44	0.30
22.4	4.77E-04	3.44	0.19	30.07	0.25	0.47	0.32
22.6	5.72E-04	3.43	0.25	24.71	0.25	0.36	0.28
22.8	7.78E-04	3.37	0.35	23.47	0.24	0.28	0.27
23.0	1.47E-03	3.15	0.46	23.36	0.24	0.19	0.26
23.2	2.29E-03	3.05	0.51	22.45	0.24	0.05	0.31

b : $R_g = \text{RHS} = 6.2$ nm

Calculation of the photo- and chemical initiation rates

The initiator decomposition rate at 70°C was calculated using the Arrhenius equation:

$$k_i = A \times e^{\left(\frac{-E_A}{RT}\right)} = 1.20 \times 10^{-4} \text{ s}^{-1}$$

With the frequency factor: $\ln(A) = 34.23$ (i.e. $A = 7.34 \times 10^{14}$). The activation energy: $E_A = 123.4 \text{ kJ mol}^{-1}$, $R = 8.314 \text{ J mol}^{-1} \text{ K}^{-1}$ and $T = 343 \text{ K}$.

The mass of initiator is 0.103 g ($3.8 \times 10^{-4} \text{ mol}$). Therefore, the flux of chemically produced radicals is $n_{R\cdot} = 2 \times n_i \times k_i = 9.13 \times 10^{-8} \text{ mol/s}$

The X-ray flux is $10^{11} \text{ photon/sec}$, considering that only 10% of the photons are adsorbed (90% being either transmitted or scattered), and assuming that each photon gives a radical (photochemical yield of 100%), this gives a flux of photo-produced radicals:

$$n_{R\cdot} = \frac{10^{-10}}{N_A} = 1.66 \times 10^{-14} \text{ mol/s}$$

REFERENCES

(S1) Galanopoulo, P.; Dugas, P.-Y.; Lansalot, M.; D'Agosto, F. Poly(ethylene glycol)-*b*-poly(vinyl acetate) block copolymer particles with various morphologies via RAFT/MADIX aqueous emulsion PISA. *Polym. Chem.* **2020**, *11*, 3922-3930.